Research Article

Min Li*, Bernhard Karpuschewski, and Oltmann Riemer

High-efficiency nano polishing of steel materials

https://doi.org/10.1515/ntrev-2021-0092
received August 29, 2021; accepted September 15, 2021

Abstract: The application of a specific rheological polishing slurry is proposed first for high-efficiency machining of steel materials to achieve high-quality ultraprecision finished surfaces. The rheology of the polishing slurry was explored to show that the non-Newtonian medium with certain parameters of content components exhibits shear-thickening behavior. Then the new high-efficiency nano polishing approach is applied to process spherical surfaces of bearing steel. Several controllable parameters such as shear rheology, abrasive data, rotational speed, and processing time are experimentally investigated in this polishing process. A special finding is that the surface roughness and material removal rate can increase simultaneously when a small abrasive size is applied due to the thickening mechanism during the shearing flow of slurries. Excessive abrasives can decrease surface quality due to the uneven agglomeration of particles scratching the surface. Under optimized conditions, a high-accuracy spherical bearing steel surface with a roughness of 12.6 nm and roundness of 5.3 μm was achieved after a processing time of 2.5 h. Thus, a potential ultraprecision machining method for target materials is obtained in this study.

Keywords: nano-polishing, ultraprecision machining, shear-thickening rheological stimulus, material removal, high efficiency slurry, high accuracy

*** Corresponding author: Min Li,** Department of Manufacturing Technologies, Leibniz Institute for Materials Engineering, 28359 Bremen, Germany; Intelligent Manufacturing Institute, Hunan University of Science and Technology, Xiangtan 411201, China; MAPEX Center for Materials and Processes/LFM, University of Bremen, 28359 Bremen, Germany,
e-mail: minli@iwt.uni-bremen.de, tel: +49-176-3460-3373
Bernhard Karpuschewski, Oltmann Riemer: Department of Manufacturing Technologies, Leibniz Institute for Materials Engineering, 28359 Bremen, Germany; MAPEX Center for Materials and Processes/LFM, University of Bremen, 28359 Bremen, Germany

1 Introduction

Precisely finished components have increasing practical applications such as aero engine blades, biomedical artificial pacemaker implants, optical multiple lenses, and bearing elements [1]. The performance of these components usually depends on form accuracy and ultra-smooth surface with low or even no subsurface damage [2]. Therefore, high-efficiency deterministic finishing method is an important factor in the entire manufacturing process.

In this sense, Jones [3] developed the computer-controlled optical surfacing (CCOS) technology to achieve the shaping of high-precision surfaces. Law *et al.* [4] developed a CCOS system for correcting form errors on aspheric surfaces and obtained a 55 mm diameter aspheric workpiece with peak-to-valley (PV) error of 662 nm and root-mean-square (RMS) of 115 nm. Some polishing methods, such as magnetorheological finishing (MRF) [5], bonnet polishing [6], and chemical mechanical polishing (CMP) [7] can successfully remove tiny amounts of material and at the same time they hardly induce fracture in the machined material. Nevertheless, the high cost of magnetorheological fluids (*i.e.*, slurries) in MRF, the embedded abrasives in the material in bonnet polishing, and the regular environmental impact of chemical slurries in CMP [8] are limitations in potential uses. Rapid polishing is associated with improving the productivity of products. Accordingly, new ultraprecision polishing methods with high efficiency/high accuracy and low cost have to be identified. In this context, Li *et al.* [9,10] proposed a novel polishing approach, that is, shear-thickening polishing (STP). During the STP process, a "flexible fixed abrasive tool" will emerge in the polishing zone between the workpiece and slurry, and a persistent shear force compels the abrasives to remove the roughness peaks. However, precise rheological control of the specific slurries will determine the machining capability of the workpiece in the STP process. Subsequently, Li *et al.* [11] developed temperature-induced gradient thickening slurries to polish lithium niobate crystals with ultra-low damages. In addition, specific polishing slurries with adapted compositions provide appropriate machinability for certain workpiece materials.

In particular, bearing steel materials have a crucial application due to their superior properties (*e.g.*, specific behavior for extreme service-environments in large strength, high strengthening elastics, toughness, and excellent anti-corrosion [12–15]). Paturi *et al.* [16] applied the artificial neural network method to research tool wear and revealed the importance of cost-effective precision machining for exploring new manufacturing methods of steel material. Jouini *et al.* [17] explored the effect of surface integrity on the fatigue life of bearing rings finished by turning and grinding and pointed out that surface accuracy is the focus of bearing manufacturing. Grzesik [18] studied the significant influence of surface topography produced by turning, grinding, honing, and isotropic finishing on the friction, fatigue, corrosion, and other functional properties, and highlighted the possibilities of generating precision surfaces with target features by some manufacturing processes. Additionally, Byrne *et al.* [19] found that dimensional accuracy and roughness could respectively achieve IT5 (Ra 0.1 μm) during the cutting process. Yao *et al.* [20,21] developed a CMP machining approach with both-sides mode for cylindrical bearing steel and obtained high-accuracy polishing surfaces. Li *et al.* [22] reported the surface integrity of bearing steel element with PV error of 0.82 μm and surface roughness Ra 4.55 nm *via* a high-efficiency polishing technique. Thus, ultraprecision polishing of bearing components with satisfying high integrity in their surfaces is an emerging field.

The novel application of high-efficiency nano polishing slurries is usually restricted by the physical–chemical properties of workpiece materials. In this study, a promising alternative of polishing slurries as one contribution is proposed for the high-efficiency machining of steel materials. The shear-thickening rheological properties of the slurry are precisely controlled to effectively remove material. Several control parameters are experimentally explored in the polishing process. Another contribution of this work focuses on the shape accuracy control of spherical workpieces. Under optimum polishing conditions, a potential ultraprecision machining method for the targeted materials is obtained in this study.

2 Experiment and measurement

2.1 Polishing concept and self-developed device

Figure 1 shows the polishing concept and self-developed experimental device. The two self-rotating workpieces

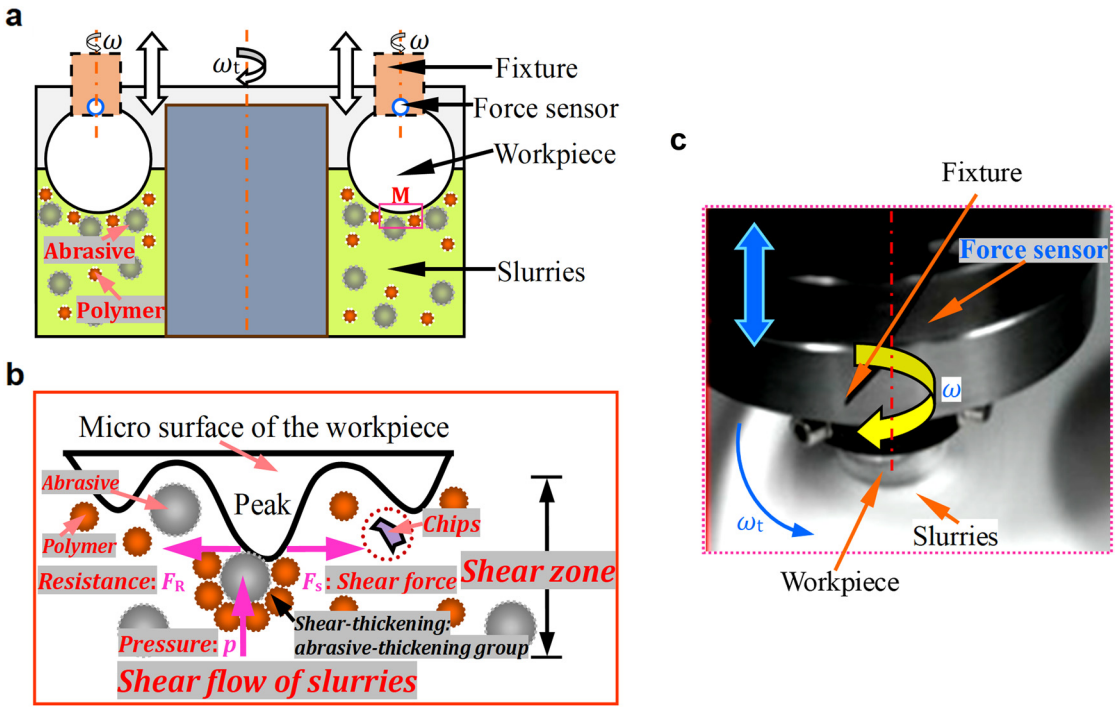

Figure 1: Schematic of the ultraprecision machining process: (a) polishing system; (b) material removal principle; (c) self-developed experimental device and magnification region M of (a).

were fixed and immersed in the new prepared slurries (*i.e.*, high-efficiency nano polishing fluids). The polishing slurries with abrasive micro-particles were prepared and added in a slurry tank with the annular groove. The liquid level depth of slurries should be controlled at 50–60 mm to facilitate greater contact with the workpiece surface. The working speed of the polishing slurry tank in Figure 1 and the controllable self-rotational speed of workpieces did not exceed 50 and 800 rpm, respectively.

In this experiment, two bearing steel parts with spherical surface (diameter: 40 mm) were selected as workpieces. The polishing conditions are shown in Table 1. The shear depth between the slurries and work is less than 1.5 mm. The effects of these controlling variables were investigated.

2.2 Preparation and rheological test

In order to obtain the high-efficiency nano polishing slurries for steel processing, the special preparation processes of these slurries should be conducted as per the following steps: first, the base liquid, which contains polymer particles (*e.g.*, polymeric substance and polyhydroxy powder) and a metal complex agent (*e.g.*, ethylene diamine tetraacetic acid) including chemical stabilizer (*e.g.*, epoxy agent) and some excipients, was prepared to achieve the important shear-thickening mechanism. Second, the abrasives Al_2O_3 with 5–35 wt% (as shown in Table 1) were added as the second phase to the above-mentioned base liquid for preparing specific slurries. Furthermore, the abrasive sizes of 1.5–15 μm in Table 1 were added in the slurries and then explored to assess the influence of the material removing mechanism for our proposed bearing steel polishing technology in this study. Finally, the components of the slurries were entirely mixed and dispersed for approx. 1 h at room temperature before the rheological test and actual polishing. Regarding the flow characteristics of slurries, a series of rheological measurements were performed with a rheometer at the same conditions and repeated three times. In addition, the states of the special slurries were observed on the KEYENCE VHX-5000 microscope. To capture the photos of the fluid state, an auxiliary device (containing slurries) with a stirring shear tool was designed under the microscope lens to provide image observation during measurements.

Table 1: Detailed experimental data

Parameters	Values
Workpiece material	Bearing component/steel
Abrasive concentration	W_a% = 5, 15, 25, 30, and 35 wt%
Abrasive size	D_a = 1.5, 3, 5, and 15 μm
Rotational speed (slurry tank)	ω_t = 45 rpm (<50 rpm)
Rotational speed (workpieces)	ω = 200–800 rpm
Shear depth	h_s = 1 and 1.5 mm
Dispersed phase	W_s% = 16, 32, and 48 wt%
Polishing time	Δt = 0.5, 1, 1.5, 2, 2.5, and 3 h

2.3 Surface characterization

The removal variation of targeting workpieces per polishing time interval were measured and calculated by a laser thickness tester (type: CMT-1100). Then the material removal mechanism and polishing quality were characterized with a profilometer (*e.g.*, the roughness and roundness accuracy of workpieces were tested by an optical profilometer and roundness testing device, respectively). Additionally, the surface micromorphology was measured by a scanning electron microscope (SEM).

3 Analysis of the rheological properties of slurries

The flow pressure (p) of slurries is always studied by flow governing formulas to ensure material removing control during bearing steel polishing. To analyze the flow conveniently, some related data should be assumed as scientific hypothesis [23,24]: (1) slurries will be assumed to be incompressible and these mediums have a certain viscosity of $\mu(\dot{\gamma})$ which depends absolutely on a scalar quantity of the shear rate; (2) the inertial force should be roughly neglected for specific fluids. The mediums are confined in the slurry tank with a gap depth of 1, 1.5 mm between the workpiece and the tank-wall. Thus, these configurations would simplify the analysis of flow control. As is known, the viscous flow developed the functional model for shear-thinning mechanism. However, in the previous work in refs [9,11], as an STP slurry, a power-law rheological condition should be determined in order to obtain a polishing effect for the workpiece machining. Moreover, ref. [9] also explored the power-law fitting curve of the rheological characteristic. Governing viscosity and shear stress in the flow field, for dramatically producing

shear-thickening mechanism, the mathematical power-law formulas [25] of polishing slurries can be expressed as:

$$\mu(\dot{\gamma}) = c \cdot \dot{\gamma}^{n-1}, \tag{1}$$

$$\tau = \mu(\dot{\gamma}) \cdot \dot{\gamma}, \tag{2}$$

$$\dot{\gamma} = v_{\Delta}/h_{\mathrm{s}}, \tag{3}$$

where $\mu(\dot{\gamma})$ is a mathematical scalar function in these equations, c represents the consistency index, especially the power-law exponent n is greater than 1; τ represents the shear stress in the flow field, and $\dot{\gamma}$ represents the shear rate which is equal to the ratio of velocity gradient (v_{Δ}) to shear depth (h_{s}). Generally, the flow viscosity $\mu(\dot{\gamma})$ commonly varies and grows with shear rates $\dot{\gamma}$ when the exponent n is greater than 1; in addition, the above-mentioned mathematical formulas are adapting the increment of $\dot{\gamma}$ under high shearing condition.

Macroscopically, the flow viscosity $\mu(\dot{\gamma})$ in equation (1) will be demonstrated as the holding force and is controlled by the strength of the "flexible fixed abrasive tool" in the polishing process. As a controllable finishing technology, effective control of polishing conditions, especially flow viscosity $\mu(\dot{\gamma})$, will play a decisive role in ensuring workpiece accuracy. Galindo-Rosales e*t al.* [26] developed a one liquid viscosity function on the shear-thickening phenomenon to present the three sections of rheology curves, for example from thinning to thickening and then to thinning behavior. Nevertheless, the research work in ref. [26] is only made available for colloidal suspensions without abrasives. Moreover, some previous research works in refs [9,11,27], indicate that the existence of abrasives in polishing slurries can generate a "flexible fixed abrasive tool" under the rheological properties to a certain extent. Thus, the flow viscosity formula can be given approximately by apparent viscosity as

$$\mu_{\mathrm{s}} = \mu_{\mathrm{m}} + \frac{\mu_{\mathrm{c}} - \mu_{\mathrm{m}}}{1 + [K_{\mathrm{s}}\dot{\gamma}(\dot{\gamma} - \dot{\gamma}_{\mathrm{c}})/(\dot{\gamma} - \dot{\gamma}_{\mathrm{m}})]^{n}}, \tag{4}$$

where $\mu_{\mathrm{s}}(\dot{\gamma})$ represents the flow viscosity in the thickening region for the polishing slurries; $\mu_{\mathrm{m}}(\dot{\gamma})$ represents the asymptotic datum of flow viscosity under the high shearing or larger shear rate $\dot{\gamma}$; and $\mu_{\mathrm{c}}(\dot{\gamma})$ represents the asymptotic datum under the extremely small shearing or shear rate $\dot{\gamma}$. Theoretically, shear thickening happens when the flow viscosity is $\mu(\dot{\gamma}) \in [\mu_{\mathrm{c}}(\dot{\gamma}), \mu_{\mathrm{m}}(\dot{\gamma})]$. Under the shear-thickening regime, the viscosities of polishing slurries are non-monotonically decided by abrasives in addition to shearing actions.

$$\mu_{\text{s-d}} = \mu_{\mathrm{c}} + \frac{\mu_{i} - \mu_{\mathrm{c}}}{1 + [K_{\text{s-d}}\dot{\gamma}^{2}/(\dot{\gamma} - \dot{\gamma}_{\mathrm{c}})]^{n_{\text{s-d}}}}, \tag{5}$$

$$\mu_{\text{s-r}} = \mu_{\mathrm{m}} + \frac{\mu_{\mathrm{c}} - \mu_{\mathrm{m}}}{1 + [K_{\mathrm{s}}\dot{\gamma}(\dot{\gamma} - \dot{\gamma}_{\mathrm{c}})/(\dot{\gamma} - \dot{\gamma}_{\mathrm{m}})]^{n_{\mathrm{s}}}}, \tag{6}$$

$$\mu_{\text{s-dp}} = \frac{\mu_{\mathrm{m}}}{1 + [K_{\text{s-dp}}(\dot{\gamma} - \dot{\gamma}_{\mathrm{m}})]^{n_{\text{s-dp}}}}, \tag{7}$$

where equations (5)–(7) have the similar mathematical form expressed in equation (4). The parameters K_i (when i = s-d, s, s-dp) express the transitions from thinning to thickening mechanism, while the power exponents n_i (when i = s-d, s, s-dp) involve three slopes for every flow transition region under different shear rates. According to the viscosities of the polishing slurries, the typical characteristics can be derived as the following:

1. Region of shear-thinning mechanism: μ_i represents the asymptotic value with the extremely small shear rates, n_i represents the curve slope for thinning mechanism; $K_{\text{s-d}}$ expresses the transitions from thinning to thickening mechanism; and $\dot{\gamma}_{\mathrm{c}}$ represents the critical value of $\dot{\gamma}$ for the thinning region.
2. Region of shear-thickening mechanism: μ_{c} represents the critical thickening-viscosity with the rising shear rates, n_{s} represents the curve slope for thickening mechanism; $K_{\text{s-d}}$ expresses the transitions from thickening to thinning mechanism; and $\dot{\gamma}_{\mathrm{m}}$ represents the critical value of $\dot{\gamma}$ for the thickening region.
3. Region of shear-thinning mechanism: μ_{m} refers to the critical thinning-viscosity with the extremely larger shear rates, $n_{\text{s-dp}}$ refers to the slope for the thinning mechanism; $K_{\text{s-dp}}$ expresses the transitions from thickening to thinning mechanism; and $\dot{\gamma}_{\mathrm{m}}$ represents the critical value of $\dot{\gamma}$ for the thinning region.

As pointed out in Section 2.1, the crucial concept of this high-efficiency nano polishing process lies in the control of the rheological mechanism in the region of shear thickening to obtain a bigger holding force on the abrasives. Thus, the viscosities of the polishing slurry should be explored and the rheological curves should be determined to find the important controllable parameters such as velocity gradient (v_{Δ}) and shear depth (h_{s}). Naturally, the velocity gradient will be decided by the rotational speed of the associated workpieces and the appropriate rotational speed of the slurry tank. More importantly, the shear depth can always be determined and adjusted by the polishing turntable. As per the Preston's equation of material removal [25], the polishing velocity (v) and pressure (p) are the two key conditions regulating polishing efficiency. Thus, the performance

control of the slurries will lay an effective foundation for subsequent material removal analysis in Section 4.

4 Analysis of material removal efficiency

As the rheological properties of polishing slurries are configured with two parameters (*e.g.*, velocity gradient, v_Δ and shear depth h_s), the polishing process will have to be regulated and controlled to ensure best machining results for workpieces. Therefore, for our polishing approach, based on the Preston's equation [28], we can express the material removal rate (MRR) equation:

$$\mathrm{MRR} = k \cdot p \cdot v_\Delta, \tag{8}$$

where k represents a coefficient related to the actual polishing conditions, p represents the polishing pressure calculated by the flow functions and the force sensor in Figure 1, and v_Δ represents the velocity gradient in the flow field of slurries.

With the detailed polishing conditions demonstrated in Table 1, all five values of MRR represented by $\mathrm{MRR_p}$ of various testing zones can be obtained in the experiments as:

$$\mathrm{MRR_p} = \Delta h/\Delta t = (h_i - h_p)/\Delta t, \tag{9}$$

where $\mathrm{MRR_p}$ represents the experimental value, Δh represents the height difference of actual removal, h_i represents the initial height, and h_p represents the machined height in our polishing process of time interval Δt.

Based on equation (8), coefficient k must be computed as per the actual polishing data of $\mathrm{MRR_p}$. With the target testing positions on bearing steel surfaces, certain differences exist regarding the actual polishing data of $\mathrm{MRR_p}$ resulting in several values of the coefficient k. After that, the mean coefficient $\bar{k}_p$ of actual polishing data will be obtained in this study. Thus, the new equation $\mathrm{MRR_f}$ for our study will be given as the following:

$$\mathrm{MRR_f} = \bar{k}_p \cdot p \cdot v_\Delta, \tag{10}$$

where $\mathrm{MRR_f}$ represents the modified model, $\bar{k}_p$ represents the average value for k in equation (8), p represents the polishing pressure, and v_Δ represents the velocity gradient.

5 Results and discussion

Figure 2 presents the rheological states of slurries in the original non-thickening condition as well as after shear thickening. In order to capture the fluid state, an auxiliary device (containing slurries) with a disturbance tool was designed under the microscope lens to provide image observation during the testing process. An external disturbance driven by shear force is more likely to produce abrasive Al_2O_3-"thickening" groups for the slurries under test. At the extreme lower shear rates ($\dot{\gamma}$), the slurries mainly present a viscous state with the liquid flow action in Figure 2a. Nevertheless, for the higher shear rates ($\dot{\gamma}$), the elastic state exhibits a solid-like action in Figure 2b. Thus, the rheological curves should be determined to realize the controllable polishing of workpieces. Figure 3 presents a series of rheological curves of our new applied polishing slurries with the Al_2O_3 abrasives. The three rheological curves related to flow-viscosities (η) and shear-rates ($\dot{\gamma}$) present similar trends approximately, that is, η rises as the consecutive growth of $\dot{\gamma}$. The critical shear thickening happens as $\dot{\gamma}$ equals to $3\,\mathrm{s}^{-1}$, while the critical shear-thinning threshold appears at the condition of $\dot{\gamma} = 100\,\mathrm{s}^{-1}$. Theoretically, the best shear zone for polishing should be controlled under the condition of

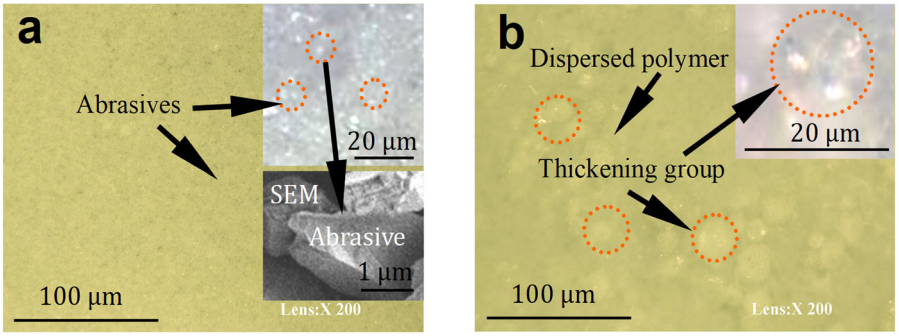

Figure 2: States of the special slurries observed on the VHX-5000 microscope and SEM: (a) initial dispersion and (b) thickening group.

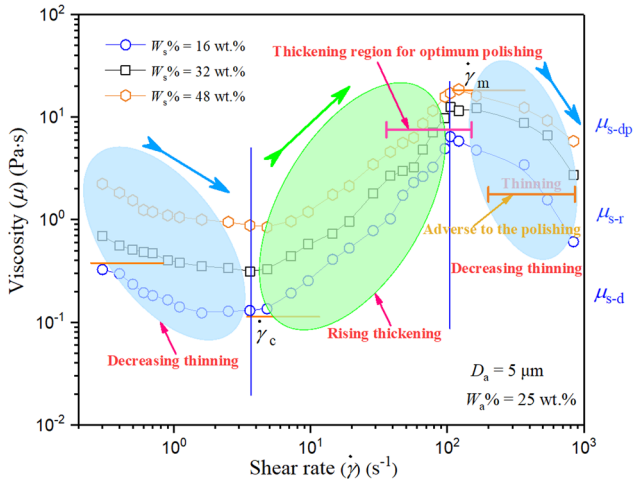

Figure 3: Three rheological curves of the experimental slurries (flow viscosity *vs* shear rate).

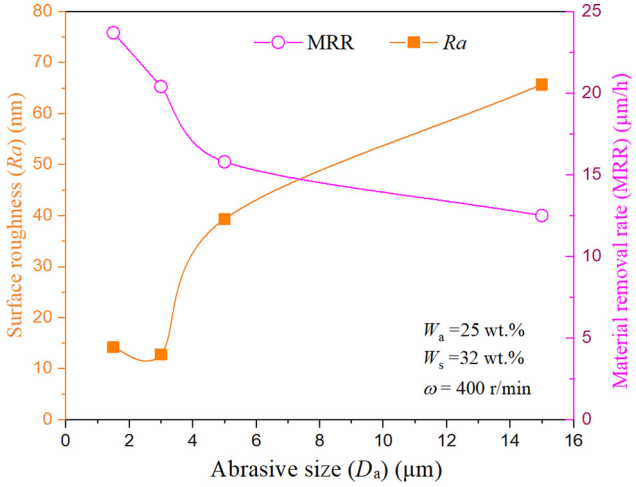

Figure 4: Influence of different abrasive size of Al_2O_3 on surface roughness Ra and MRR.

$\dot{\gamma} \in [100, 200]\ s^{-1}$, so that the sufficient holding force on the abrasives will result in high-efficiency material removal.

As shown in Figure 3, the prepared polishing slurries exhibit non-Newtonian flow features of shear-thickening rheology. According to the viscosities of the polishing slurries, the typical characteristics can be derived as three regions: (1) region of shear-thinning mechanism; (2) region of shear-thickening mechanism; and (3) region of shear-thinning mechanism. Theoretically, at extremely low shear rates $\dot{\gamma}$ of the first region in Figure 3, the specific construction of the polymer-chains in the slurries moves at a slow speed and its entanglement does not prevent the shearing flow [29]. Then, for the second region in Figure 3, an appropriate thickening region of the shear action is controlled for the polishing of the spherical bearing steel. In addition, for the third region in Figure 3, the shear-thinning phenomenon may have resulted from disentanglement of the polymer-chains during the shearing flow. More importantly, for the second region of rheological slurries, when $\dot{\gamma}$ reaches the threshold of thickening (*e.g.*, μ_c in equation (6)), the viscosities of our applied slurries unexpectedly increase and the drag force of liquid flow around the work surfaces rises at high axial pressure. Thus, the specific variation results in thickening phases to generate some clusters or groups, driving micro-cutting abrasives to generate elastic polymers–abrasives clusters (Figure 2b). Therefore, the mechanical removal processes for polishing rose at tiny surface rough peaks on the spherical bearing steel parts.

Figure 4 demonstrates the influence of abrasive size (D_a) on the polishing of workpieces. During the polishing process, as shown in Figure 4, the abrasive size D_a of Al_2O_3 has a great effect on the variation of workpiece's roughness Ra (unpolished surface of Ra 310.0 nm). The polished surface demonstrated mirror-like smoothness with surface roughness Ra (12.8 nm) under the conditions of abrasive size D_a = 3 μm, ω = 700 rpm, W_s% = 32 wt%, and W_a% = 25 wt%. With the abrasive size (D_a) decreasing from 15 to 1.5 μm, the surface quality of the spherical bearing steel parts improved during the polishing process. The number of abrasives in the slurries increases with decreasing particle size. Thus, with constant Al_2O_3 concentration, the roughness Ra of spherical parts decreases more rapidly. In Figure 4, the surface roughness increases dramatically when D_a > 3 μm, which can be explained theoretically with the explanation that a large size abrasive will cause large scratches on the workpiece surface [9], resulting in the mutation of surface roughness Ra. Moreover, the abrasive size of Al_2O_3 can affect the construction of the elastic polymers–abrasives clusters, and then this abrasive Al_2O_3-"thickening" groups generate the micro-cutting of the workpieces. The control of the abrasive size made a crucial contribution in improving the roughness Ra of the workpieces. The MRR has a little variation with the abrasive size due to the ratio of D_a to particle size of the thickening phase. However, the research result in Figure 4 shows a special finding that Ra and MRR can increase simultaneously during the application of small abrasive size D_a due to the thickening mechanism during the shearing flow of slurries. Theoretically, at the same concentration of abrasives in slurries, MRR reduces with the increase in the abrasive size D_a. It might be decided by the smaller number of abrasives and smaller micro-cutting edge in the polishing contacting zone. In addition, the scratches/pits and damages on initial rough surfaces (Figure 5a) would be rapidly deburred (Figure 5b) and reduced due to

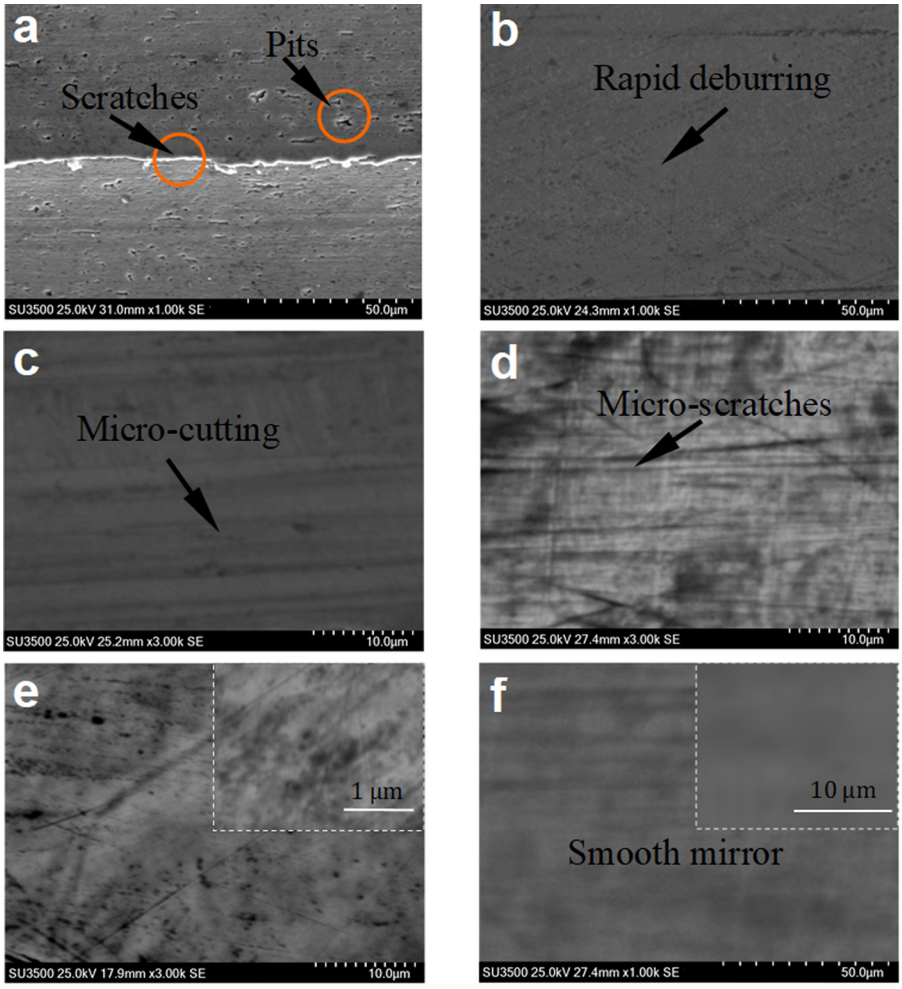

Figure 5: Surface micromorphology: (a) unpolished rough surface with scratches (0 h); (b) rapid deburring (0.5 h); (c) micro-cutting (1 h); (d) generation of micro-scratches (1.5 h); (e) surface flattening (2 h); and (f) polished smooth mirror (2.5 h).

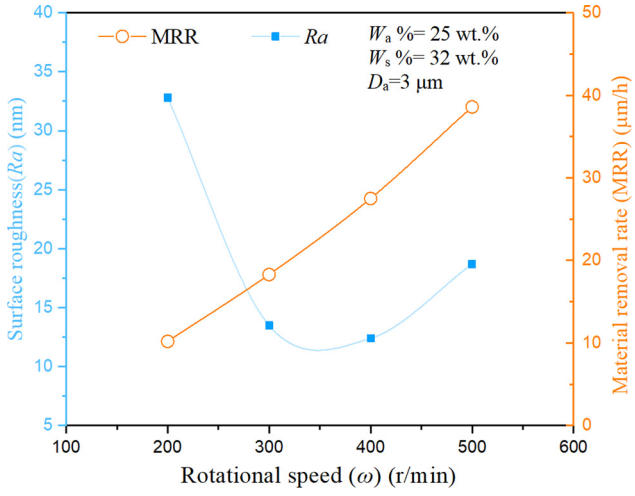

Figure 6: Effect of self-rotational speed of workpieces ω on the polishing data of Ra and MRR.

the micro-cutting action of abrasives (Figure 5c). When the polishing process continues, the surfaces of workpieces can gradually flatten as shown in Figure 5d and e. Finally, smooth spherical surfaces were achieved in this process (Figure 5f).

Figure 6 demonstrates the influence of the self-rotational speed of workpieces. As the self-rotational speed of workpiece (ω) increases at the constant rotational speed of slurry tank ω_t = 45 rpm, the thickening mechanism exhibits a higher intensity than at low speed, and then the shear stress will grow rapidly to reach large material removal. As the self-rotational speed of workpieces (ω) equals to 400 rpm and the rotational speed of slurry tank ω_t = 45 rpm, the roughness will reduce to Ra 12.4 nm at the polishing time of 3 h. Meanwhile, once the rheological feature of the slurries with the region of rising thickening reaches the thickening region of optimum polishing, as shown in Figure 3, the appropriate shear

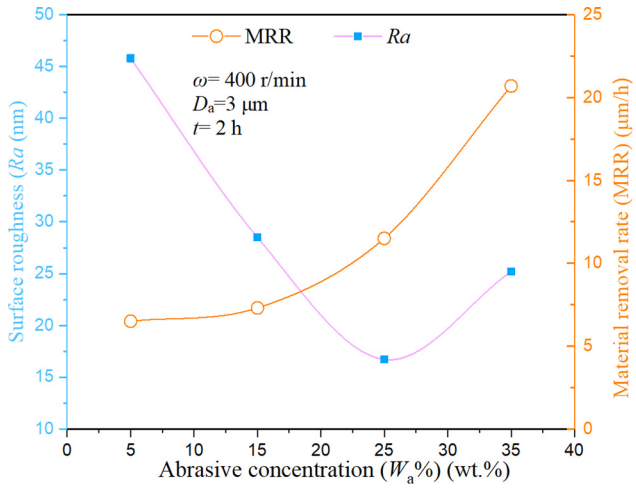

Figure 7: Effect of Al_2O_3 concentration on polishing data of Ra and MRR.

action of thickening phases can be controlled to generate some clusters or groups, driving micro-cutting abrasives to generate elastic polymers–abrasives clusters for the workpiece polishing. Excessive rotational speed (>400 rpm) can affect the formation of the optimal thickening region and will reduce surface quality with the increasing of surface roughness. These results reveal the removal capability of the effective flexible "polymer-abrasive clusters." This is a remarkable improvement caused by the sharp strengthening of the shear-thickening mechanism. Therefore, once more rough peaks on the targeting surfaces are selectively cut in the polishing time per trial, the polishing quality should be dramatically improved with increasing MRR.

Figure 7 demonstrates the influence of abrasive concentration (W_a%). The change of the roughness is always decreasing when W_a% < 25 wt%. However, when W_a% > 25 wt%, the roughness will increase and will lead to a deterioration of surface quality of spherical bearing steel surfaces. Under the critical abrasive concentration of W_a% = 25 wt%, Ra reaches 16.7 nm in 2 h. According to polishing theories, at lower Al_2O_3 concentration W_a%, only a few abrasives are involved in the micro-removing of workpieces. As a result, an ideal processing effect with high MRR and low surface roughness cannot be achieved. A rising concentration causes the growth of effective abrasives in material micro-removing and produces more rapid material removal and a slighter decrease of roughness [30]. However, excessive abrasives can reduce surface quality due to the uneven agglomeration of particles scratching the surface. The polished surfaces have presented certain differences with various abrasive sizes. The surface roughness of the workpiece can be reduced from Ra 310 to 16.7 nm at an optimum Al_2O_3 concentration of W_a% = 25 wt%.

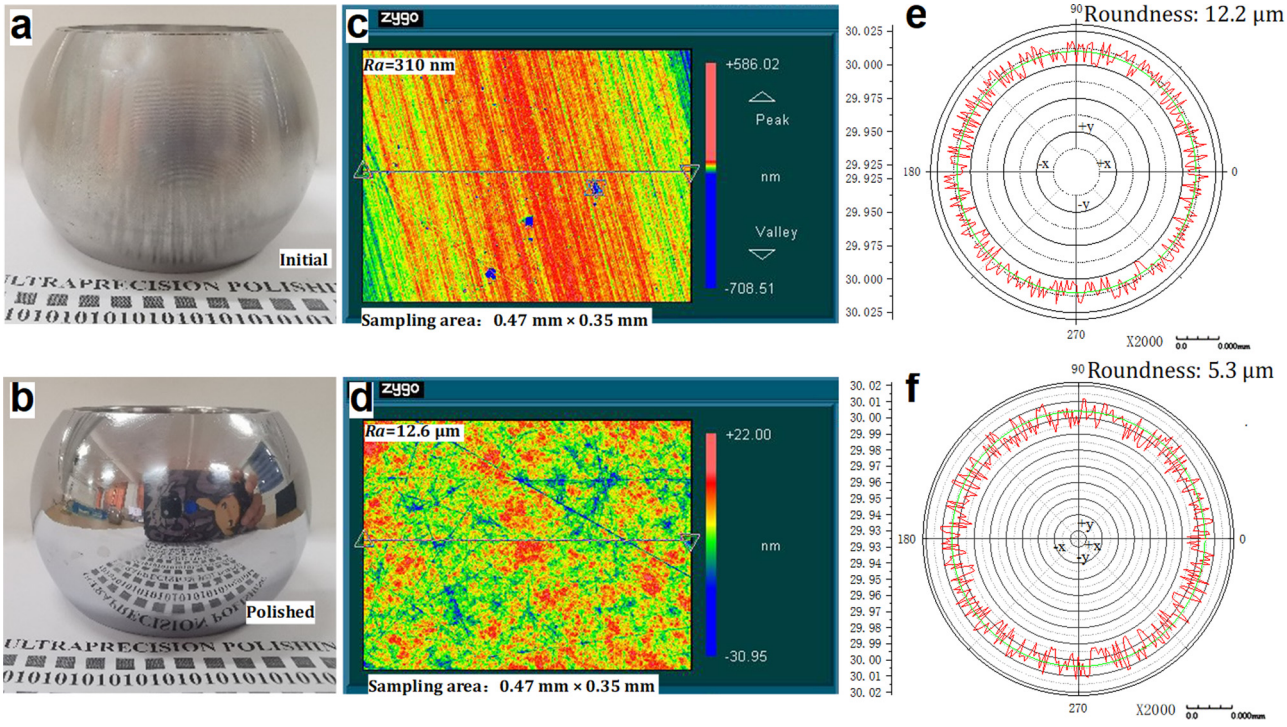

Figure 8: Comparison of the initial and polished surface quality: (a) initial work piece; (b) polished work piece (2.5 h); (c) initial surface with scratches; (d) polished work piece (2.5 h); (e) roundness of the initial work piece; and (f) roundness of the polished work piece (2.5 h).

Figure 8 demonstrates the workpiece after a 2.5 h polishing process. Under the optimized experimental process conditions of D_a = 3 μm, ω = 400 rpm, W_a% = 25 wt%, the surface roughness of the spherical bearing steel component reduced from Ra 310 (in Figure 8a and c) to 12.6 nm, and a smooth-like surface was obtained in Figure 8b–d. The material removal mechanism would be a continuous process of micro-cutting [31–33], resulting in removing scratches and pits to demonstrate "flexible polishing" [34–36] on the target surfaces. These research findings indicate that material surface defects were greatly reduced during the proposed polishing. More importantly, the optimization of processing parameters can be helpful to control some other intermediate or uncertain factors [37], so as to improve the actual polishing accuracy of workpieces in this study. In addition, shape accuracy is an essential polishing datum for curved surfaces and can affect the component assembly process and practical application of the final product. Figure 8e and f demonstrate the roundness variation of the workpiece before and after polishing. The roundness value of the curved surface parts improves obviously after a polishing time of 2 h, and the roundness declines steadily from 12.2 to 5.3 μm after a processing time of 2.5 h. Moreover, due to the limitation of polishing conditions in this work, excessive polishing time (*i.e.*, 3 h) cannot significantly improve the surface quality of workpieces. Actually, if we further regulate the abrasive shape [11] or composition of slurries [38], it might shorten the processing time (e.g. $\Delta t < 2h$), which is expected to further improve the processing efficiency of workpieces. The research reveals that the high-efficiency nano polishing process is a valuable ultraprecision machining approach for spherical bearing steel components.

6 Conclusion

A potential ultraprecision machining technology for specific steel materials was proposed in this study. The following conclusions were drawn from this study.

The specifically prepared high-efficiency nano polishing slurries exhibit non-Newtonian flow features of shear-thickening rheology. Further, the shear-thickening rheological properties of the slurry can be precisely controlled to achieve material removal. As the rotational speed increases at a constant rotational speed of the slurry tank, the thickening mechanism at high rotational speed shows much higher intensity than that in low rotational speed, and the shear stress will grow rapidly to effect large material removal due to the formation of flexible "polymer–abrasives clusters." The control of the abrasive size made a crucial contribution in improving the surface roughness Ra of workpieces. A special finding is that Ra and MRR can increase simultaneously when small abrasive size D_a is applied due to the thickening mechanism during the shearing flow of slurries. The change of the roughness is always decreasing when W_a% < 25 wt%. However, when W_a% > 25 wt%, the roughness will increase and will lead to a deterioration of surface quality of spherical bearing steel surfaces. Excessive abrasives can decrease the surface quality due to the uneven agglomeration of particles scratching the surface. Under the optimized experimental process conditions of D_a = 3 μm, ω = 400 rpm, and W_a% = 25 wt%, the roughness of the spherical parts decreased from Ra 310.0 to 12.6 nm, and the roundness improved from 12.2 to 5.3 μm after a processing time of 2.5 h. Thus, the high-efficiency nano polishing process is an ultraprecision machining approach with good prospects for producing high-accuracy spherical bearing steel components.

Acknowledgments: The authors would like to acknowledge Zhenrong Huang and Jiancheng Xie from China for their experimental assistance in measurement and materials.

Funding information: This research was funded by the Alexander von Humboldt Foundation (AvH), Germany; and the Hunan Provincial Key R & D Project (Grant number 2017GK2050), China.

Author contributions: All authors have accepted responsibility for the entire content of this manuscript and approved its submission.

Conflict of interest: The authors declare no conflict of interest.

References

[1] Achour SB, Bissacco G, Beaucamp A, Chiffre LD. Deterministic polishing of micro geometries. CIRP Ann. 2020;69(1):305–8.
[2] Lucca DA, Brinksmeier E, Goch G. Progress in assessing surface and subsurface integrity. CIRP Ann. 1998;47(2):669–93.
[3] Jones RA. Computer-controlled optical surfacing with orbital tool motion. Opt Eng. 1986;25(6):256785.
[4] Law PL, Messelink WACM, Weber R. Development of a cost-efficient computer controlled optical surfacing process for correcting aspheric lenses using tool influence function based

dwelltime optimization. EPJ Web Conf. 2019;215:01002. doi: 10.1051/epjconf/201921501002.
[5] Menapace JA, Davis PJ, Steele WA, Hachkowski MR, Nelson A, Xin K. MRF applications: on the road to making large-aperture ultraviolet laser resistant continuous phase plates for high-power lasers. Proceedings of SPIE – The International Society for Optical Engineering; 25–27 September 2006. Boulder, Co, USA: SPIE; 2006. p. 64030N. doi: 10.1117/12.696329.
[6] Namba Y, Beaucamp A, Freeman R. Ultra-precision polishing by fluid jet and bonnet polishing for next generation hard x-ray telescope application. Proceedings – ASPE 2010 Annual Meeting; 2010. p. 50.
[7] Coutinho CA, Gupta VK. Chemical mechanical polishing: role of polymeric additives and composite particles in slurries. In: Myer Kutz, editor. Applied plastics engineering handbook; plastics design library. New York: William Andrew Publishing; 2011. p. 519–32.
[8] Zhao G, Wei Z, Wang W, Feng D, Xu A, Liu W, et al. Review on modeling and application of chemical mechanical polishing. Nanotechnol Rev. 2020;9(1):182–9.
[9] Li M, Lyu B, Yuan J, Dong C, Dai W. Shear-thickening polishing method. Int J Mach Tool Manuf. 2015;94:88–99.
[10] Li M, Lyu B, Yuan J, Yao W, Zhou F, Zhong M. Evolution and equivalent control law of surface roughness in shear-thickening polishing. Int J Mach Tool Manuf. 2016;108:113–26.
[11] Li M, Karpuschewski B, Ohmori H, Riemer O, Wang Y, Dong T. Adaptive shearing-gradient thickening polishing (AS-GTP) and subsurface damage inhibition. Int J Mach Tool Manuf. 2021;160:103651.
[12] Schwack F, Bader N, Leckner J, Demaille C, Poll G. A study of grease lubricants under wind turbine pitch bearing conditions. Wear. 2020;454–455:203335.
[13] Mahajan S. In: Buschow KHJ, Cahn R, Flemings M, Ilschner B, Kramer E, Mahajan S, et al. editors. Encyclopedia of materials: science and technology. 1st edn. Amsterdam: Elsevier; 2001.
[14] Panda A, Sahoo AK, Kumar R, Das RK. A review on machinability aspects for AISI 52100 bearing steel. Mater Today: Proc. 2019;23(3):617–21.
[15] Lyu B, Dong C, Yuan J, Sun L, Li M, Dai W. Experimental study on shear thickening polishing method for curved surface. Int J Nanomanuf. 2017;13(1):81–95.
[16] Paturi UMR, Cheruku S, Pasunuri VPK. Modeling of tool wear in machining of AISI 52100 steel using artificial neural networks. Mater Today: Proc. 2021;38(5):2358–65.
[17] Jouini N, Revel P, Thoquenne G. Influence of surface integrity on fatigue life of bearing rings finished by precision hard turning and grinding. J Manuf Process. 2020;57:444–51.
[18] Grzesik W. Prediction of the functional performance of machined components based on surface topography: state of the art. J Mater Eng Perform. 2016;25:4460–8.
[19] Byrne G, Dornfeld D, Denkena B. Advancing cutting technology. CIRP Ann. 2003;52(2):483–507.
[20] Yao W, Yuan J, Zhou F, Chen Z, Zhao T, Zhong M. Trajectory analysis and experiments of both-sides cylindrical lapping in eccentric rotation. Int J Adv Manuf Tech. 2017;88:2849–59.
[21] Yao W, Lyu B, Wang C, Fei X, Zhang L. Modeling, simulation, and experimental verification on material removal and rounding process of centerless cylindrical finishing with free abrasives and soft pad. Int J Adv Manuf Tech. 2021;114:1443–55.
[22] Li M, Huang Z, Dong T, Mao M, Lyu B, Yuan J. Surface integrity of bearing steel element with a new high-efficiency shear thickening polishing technique. Proc CIRP. 2018;71:313–6.
[23] Nejat A, Jalali A, Sharbatdar M. The flow of Newtonian and power law fluids in elastic tubes. J Non-Newtonian Fluid Mech. 2011;166:1158–72.
[24] Manica R, Bortoli AD. Simulation of sudden expansion flows for power-law fluids. J Non-Newtonian Fluid Mech. 2004;121:35–40.
[25] Mendes PRS, Dutra ESS. Viscosity function for yield-stress liquids. Appl Rheol. 2004;14:296–302.
[26] Galindo-Rosales FJ, Rubio-Hernández FJ, Sevilla A. An apparent viscosity function for shear thickening fluids. J Non-Newton Fluid Mech. 2011;166:321–5.
[27] Li M, Liu M, Riemer O, Karpuschewski B, Tang C. Origin of material removal mechanism in shear thickening-chemical polishing. Int J Mach Tool Manuf. 2021;170:103800.
[28] Preston F. The theory and design of plate glass polishing machines. J Soc Glas Technol. 1927;11:214–56.
[29] Graham RS, Likhtman AE, McLeish TCB, Milner ST. Microscopic theory of linear, entangled polymer chains under rapid deformation including chain stretch and convective constraint release. J Rheol. 2003;47:1171–200.
[30] Li M, Liu M, Riemer O, Song F, Lyu B. Anhydrous based shear-thickening polishing of KDP crystal. Chin J Aeronaut. 2021;34(6):90–9.
[31] Hashimoto F, Yamaguchi H, Krajnik P, Wegener K, Chaudhari R, Hoffmeister HW, et al. Abrasive fine-finishing technology. CIRP Ann. 2016;65:597–620.
[32] Mathew PT, Rodriguez BJ, Fang F. Atomic and close-to-atomic scale manufacturing: a review on atomic layer removal methods using atomic force microscopy. Nanomanuf Metrol. 2020;3:167–86.
[33] Matsukuma H, Wen B, Osawa S, Gao W. Design and construction of a low-force stylus probe for on-machine tool cutting edge measurement. Nanomanuf Metrol. 2020;3:282–91.
[34] Li M, Yuan J, Lü B. Preparation of shear thickening polishing abrasive slurries and their polishing properties. Opt Precis Eng. 2015;23(9):2513–21.
[35] Li M, Lü B, Yuan J, Dong C, Dai W. Material removal mathematics model of shear thickening polishing. J Mech Eng. 2016;52(7):142–51.
[36] Li M, Huang Z, Dong T, Tang C, Lyu B, Yuan J. Surface quality of Zirconia (ZrO_2) parts in shear-thickening high-efficiency polishing. Proc CIRP. 2018;77:143–6.
[37] Yuan J, Mao M, Li M, Liu S, Wu F, Yuan J, Hu Z, et al. Optimization of CMP processing parameters for YG8 cemented carbide inserts based on RSM. Chin Mech Eng. 2018;29(19):2290–7.
[38] Mao M, Xu Q, Liu J, Yuan J, Li M, Hu Z. Contact states of workpiece-abrasive particles-polishing pad in cemented carbide CMP processes. Chin Mech Eng. 2018;32(17):2074–81.